# Wireless Gas Leak Detection and Localization

Fabien Chraim, Yusuf Bugra Erol, and Kris Pister

***Abstract*—Thousands of industrial gas leaks occur every year, with many leading to injuries, deaths, equipment damage, and a disastrous environmental effect. There have been many attempts at solving this problem, but with limited success. This paper proposes a wireless gas leak detection and localization solution. With a monitoring network of 20 wireless devices covering 200 $m^2$, 60 propane releases are performed. The detection and localization algorithms proposed here are applied to the collected concentration data, and the methodology is evaluated. A detection rate of 91% is achieved, with seven false alarms recorded over 3 days, and an average detection delay of 108 s. The localization results show an accuracy of 5 m. Recommendations for future explosive gas sensor design are then presented.**

***Index Terms*—Distributed detection, gas leak detection, industrial wireless, low power networks, propane.**

## I. Introduction

THE NUMBER of gas leaks that occur every year on industrial plants is unknown. Most of these leaks, even if detected, go unreported when they do not directly lead to tangible accidents. Environmental Protection Agency (EPA) reports estimate that in the United States alone, these plants emit close to one billion cubic meters of methane (not taking any other gas into consideration). Most of these losses (around 80%) seem to come from leaky compressors, valves, seals, and connectors [1]. In 2012, approximately 2200 million metric tons of $CO_2$ equivalent were accidentally released from petroleum systems and other chemical processes necessary for the production of plastics, cement, iron, and steel [2]. It is estimated that around 800 000–900 000 leaks are investigated each year on refineries, with between 200 and 300 of them having directly resulted in loss of life, injuries, damaged equipment, or operational losses [3]. In short, industrial gas leaks present a major challenge in the quest for safe, environmental-friendly, and cost-effective plants.

In this paper, we present a distributed wireless sensor approach to the problem of gas leaks in large industrial spaces (chemical plants, refineries, oil rigs, etc.). The objective is to detect and localize "refinery-like" gas leaks within seconds of their occurrence. With many corporations upgrading their facilities with a low-power wireless infrastructure (WirelessHART) [4], a leak-detection system that simply connects to the wireless umbrella would be a desired addition to the existing safety framework. Our goal is to study the feasibility of such an approach, while carefully reviewing some of the detection challenges in the hope for opening the door for widespread commercial adoption.

This paper is organized as follows. In Section II, we will review some of the available solutions to the problem at hand, both at the academic level and commercially. Our approach is then presented in Section III, where we look at the system architecture, the hardware, and the detection/localization algorithms. Our experimental results are shown in Section IV, in which we validate our approach using real propane leaks. Future directions and recommendations are left for Section V where we conclude.

Manuscript received September 03, 2014; revised December 06, 2014 and January 20, 2015; accepted January 23, 2015. Date of publication February 02, 2015; date of current version March 29, 2016. This work was supported by Chevron Energy Technology Company and Chevron Information Technology Company. Paper no. TII-14-0978.

F. Chraim and K. Pister are with the Berkeley Sensor and Actuator Center (BSAC), University of California, Berkeley, CA 94720 USA (e-mail: chraim@eecs.berkeley.edu; pister@eecs.berkeley.edu).

Y. B. Erol is with the Center for Information Technology Research in the Interest of Society (CITRIS), University of California, Berkeley, CA 94720 USA (e-mail: yberol@eecs.berkeley.edu).

Color versions of one or more of the figures in this paper are available online at http://ieeexplore.ieee.org.

Digital Object Identifier 10.1109/TII.2015.2397879

## II. Literature Review and State of the Art

The review presented in this section is divided into a survey of commercial methods for leak detection, and some of the ideas coming out of academia.

### A. Gas Leak Detection Systems

Conventional leak detection methods fall under two categories: 1) fixed instrumentation; and 2) mobile sensing. In the former, a sensor is affixed in the general vicinity of equipment suspected of leaking (valves, compressors, etc.). These instruments are usually connected to a constant power source and generate alarms based on their sampled data. These alarms can be visual or audible, or can feed directly into a plant management system. Mobile sensors are usually hand-held devices that a worker has to point at the suspected leak source and evaluate the readings on the spot. Reports of the measurements are relayed in real time either through a wireless connection or by direct communication between the worker and other plant employees. Both these methods have their advantages and disadvantages, and most often, a hybrid system of fixed and mobile sensors is implemented. In particular, a fixed sensor is able to continuously monitor an area, as opposed to a worker who samples the same region for a few seconds perhaps before moving on. Fixed sensors have better instruments by virtue of the fact that they are less constrained, but mobile sensors allow the operator to trace a leak to its origin. It is obvious that mobile sensors put the worker at risk during the sampling process, whereas the fixed sensors enable safer operation [5].

In this study, we are only interested in fixed instruments because our proposed solution is static in nature. We now look at some of the commercially available solutions for comparison. Many solutions have been proposed for the problem of

leak detection in pipelines [6]. This topic, though relevant, is not of direct interest here, since leak detection near pipelines can be accomplished by deploying a series of sensors in a linear sequence. The solution presented in this paper would not be very practical for long pipeline installations due to the high number of sensors it would require.

Perhaps, the most prevalent leak detection methodology is by concentration measurement. Pellistor, electrochemical, semiconductor, and infrared sensors are all used to sample the ambient gas for particular species. By means of preset threshold detection, alarms are raised alerting workers and plant operators [7]. These widely adopted sensors, however, suffer from one or more of the following: low sensitivity, short lifetime, high energy consumption, sensitivity to ambient conditions, high costs, drift, etc. Typically, these sensors are operated independently, meaning that no information about the source of the leak is given. Due to the fact that they consume a considerable amount of energy, installing them becomes an issue as virtually always, the cost of laying cables outstrips the cost of the device itself [7].

Pipeline diagnosis systems gave rise to ultrasonic sensors, which have recently been adopted in some plants. The principle of operation relies on the fact that gas leaks sometimes come from punctured pipes, which emit acoustic "tone" signals in the ultrasonic band [8]. These sensors, though unaffected by environmental conditions, do not measure the intensity of the leak, and are still unable to determine its origin. They are designed to work with gases under pressure, and do not represent a general solution to industrial gas leaks.

In recent years, camera systems have found their way to the gas leak detection and localization market. These devices tend to be mounted on elevated towers, often rotating to cover the entirety of the plant. They operate by taking snapshots of the environment, then analyzing the sampled images to detect gas leaks [9]. Most of the available solutions on the market operate in the infrared band, but recently, more versatile snapshot hyper-spectral instruments are being utilized.

Energy and cost present challenges for large-scale deployments of gas sensors. Some studies have focused on improving the sensing methodology to address these issues [10], [11]. So *et al.* [10] present an optically based gas detector for various species. Their solution is based on commercial off-the-shelf components, and employs photo-acoustic spectroscopy making it tunable to various species. Their results are promising, as they achieve a reduction in power consumption as well as a reduced manufacturing cost. They validate their sensor experimentally with $CO_2$, measuring concentrations down to 410 ppb. Their designs demonstrate a $2000 device with current consumption on the order of 70 mA [10].

Somov *et al*. [11] deployment develop a hazardous gas detection system based on wireless battery-powered devices. Their methane sensor is a planar catalytic one built on gamma alumina membranes. Their circuitry achieves a reduced power consumption. Their boiler room deployment consists of nine wireless methane sensors and a gateway. The average power consumption of their device is at 2.64 mW, with a sampling interval of 30 s and a transmission every 5 min. As a result, the lifetime of their device is at 641 days. Their application targets gas sensing resolutions of 0.15% volume of methane.

### B. Detection and Localization Using Multiple Sensors

Academically, the problem of detecting and localizing leaks has been addressed in many fields. Under different names, similar methodologies have been applied in detecting the location of a speaker using many microphones, localizing objects using multiple radar streams, etc. We now list a few relevant examples.

Nofsinger *et al*. propose using inverse diffusion modeling to localize leaks. By assuming a Fickian diffusion model, they consider a large network of sensors surrounding the source of the leak. Coupling diffusion with ensemble Kalman filtering allows them to estimate the location of the source of the leaks. Their simulated system reports plume origins as numerous hypotheses each having likelihoods [12].

Huseynov *et al*. [13] propose a distributed network of microelectromechanical systems (MEMS) ultrasonic sensors for gas leak localization. In their study, a comparison of energy-decay (ED) and time-difference of arrival (TDOA) methods for localization is presented. With a distributed network of four devices, they attempt to localize a nitrogen leak from a small orifice. They employ maximum likelihood (ML) and the least squares (LS) techniques to find closed-form solutions for the diffusion differential equations. In their deployment, a 20 ft $\times$ 20 ft room is instrumented with four MEMS microphones (running at 200 kHz). Nitrogen gas was released at 150 psi at four different locations. They successfully localize the nitrogen leak with an accuracy lower than 1 ft.

Weimer *et al*. consider gas leaks in wide and dense wireless sensor networks. The problem being addressed is one of the large-scale leaks, with high concentration of gases (such as harmful gases in a metropole). In their model, therefore, they take diffusion and air currents into account. An interesting idea is presented concerning the subsampling of sensors, which are in close proximity, to reduce the network-wide energy consumption. A wake-up process ensures that all the devices are running when needed. Their method combines binary hypothesis testing with Kalman filtering, and is implemented on a testbed of 30 wireless light sensors [14].

The methods presented in these articles (and more on the topic of gas leak detection and localization) have merit, as they present valid and interesting theoretical ideas and simulations. However, they all leave much to be desired in the space of experimental validation. In this study, we attempt to solve the problem of gas leak detection and localization in the most applied manner possible. We employ some mathematical and statistical tools, and apply them to real gas concentration measurements recorded during a series of intentional releases performed in a typical industrial setting.

## III. A Wireless Distributed Sensing Approach

In this paper, we study the problem of gas leak detection and localization by means of a wireless, distributed network of sensors. Though such an approach could be viewed as a

standalone system of sensors, it could also benefit from further integration. The gas sensors utilized here could be tacked on to other industrial process control instruments. For example, the wireless valve positioning solution presented in [15] could be augmented with a gas leak sensor, as both of these problems are often linked. Furthermore, a wireless perimeter security solution [16] could also assist in detecting and localizing plant leaks as soon as suspicious concentrations leave the enclave of the plant. In this paper, we consider the leak detection solution as a stand-alone system.

### A. Hardware

As is customary with most wireless sensing applications, the hardware we developed in this study includes a radio, a microcontroller, a sensor, and a power source. Recently, the push for higher integration in the industry resulted in system-on-chip (SoC) solutions for the microcontroller and radio. In this project, the Linear Technology LTP5902 SmartMesh WirelessHART Mote Modules were utilized. They feature a 32-bit ARM Cortex M3 microcontroller, along with a 2.4-GHz, IEEE 802.15.4, WirelessHART (IEC62591) compliant radio. Combining the time-synchronized channel hopping protocol with extremely low transmission and reception power levels (on the order of 5 mA at 3 V), these modules achieve a 99.999% network reliability with a sub- 50 μA average currents.

In this project, the focus is on explosive gases. For this reason, all of the studies and releases were performed around propane, which is a by-product of natural gas processing and appears in the process of refining petroleum. This gas is the representative of the family of explosive gases, and was made available to us for use in the various experimental stages. Propane is commonly used in commercial and residential applications, and is in the liquefied petroleum (LP) gases family. As such, a propane sensor needed to be integrated with the LTP5902 SoC. The dynament premier infrared hydrocarbon (propane) sensor (MSH-P/HC/NC/5/V/P) was selected, with a 0%–2% volume measurement range [or 0–20 000 part per million (ppm)] and a resolution of 0.01% volume (100 ppm). Our integrated device is shown in Fig. 1. Though this propane sensor is, at the time of writing, one of the best on the market, its performance leaves a lot of room for improvement. For starters, it consumes an average of 80 mA of current (at 3 V), and possesses a start-up time of 1 min. This certainly represents a challenge in battery-operated devices. Additionally, the sensor has a temperature compensation routine to account for changes in the ambient temperature. However, this feature does not have a very fast response time. This means that in outdoor installations especially, small gusts of wind, which lead to temperature changes, can result in large variations in the concentration measurement (by hundreds of ppms). Although the sensor features an internal temperature reading, this measurement itself does not represent the ambient temperature around the housing of the sensor. Rather, this reading is largely affected by the heating elements inside the sensor. The response of two identical sensors deployed outdoors in the vicinity of a leak source is shown in Fig. 2. It is clear that the state-of-the-art propane sensors still present many challenges, and we hope to demonstrate that they are the missing link in the productization of this solution.

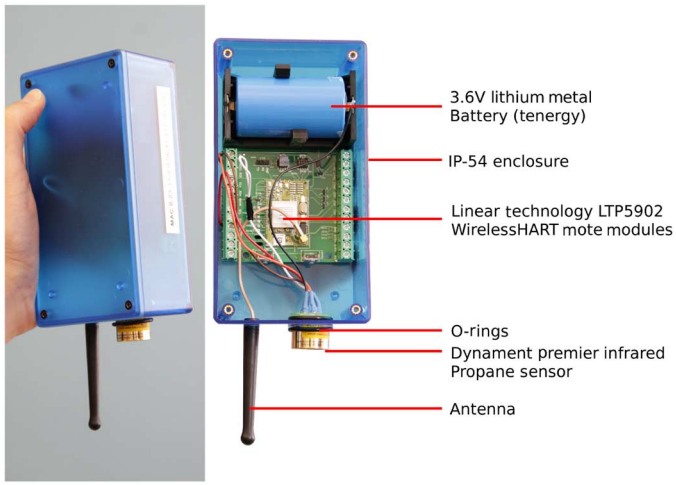


Fig. 1. Hardware platform used in this study: a wireless, battery-powered propane sensor.

Considering the average power levels of the communication module, and with careful application design and network configuration, it is often possible to implement wireless sensing applications where lifetimes extend beyond the shelf life of batteries (around 10 years). However, in this wireless gas leak application, the sensor remains as the limiting factor and a burden on the energy budget. Finally, it is worth noting that the hardware was powered by an industrial D-size lithium metal battery, with 19 Ah of charge (with a duty-cycling of 25%, this battery would hold enough charge for about 40 days). The device was enclosed in an ABS plastic IP-54 enclosure by Hammond.

### B. System Architecture

The system architecture for the leak detection solution is perhaps best explained with a picture (see Fig. 3). Taking a refinery for the sake of example, gas leak detection sensors would be deployed throughout a refinery. Though a grid distribution is often easier to manage, it is not a required feature. Indeed, these easy-to-install sensors can be mounted in seconds to the existing buildings and poles, and as long as their location is recorded, the concentration data will be easily processed by the algorithms presented later. The path from data to decision starts with concentration measurements at the node side, which are filtered and transmitted to the gateway (when needed), using the wireless infrastructure. The gateway algorithms then collect the concentration data from many sensor devices on the grounds and generate alarms whenever a leak is detected. Additionally, periodic reports concerning the concentration gradients of gases on the refinery can be generated and sent to concerned parties.

In terms of sensor placement, these devices would be spread throughout the plant. However, it is beneficial to increase the density in zones susceptible to leaks. For example, an increase in the number of compressors and valves raises the risk of leaks. As such, a typical deployment would have a minimum density necessary for detections, and then certain areas would be characterized with clusters of sensors (increased density)

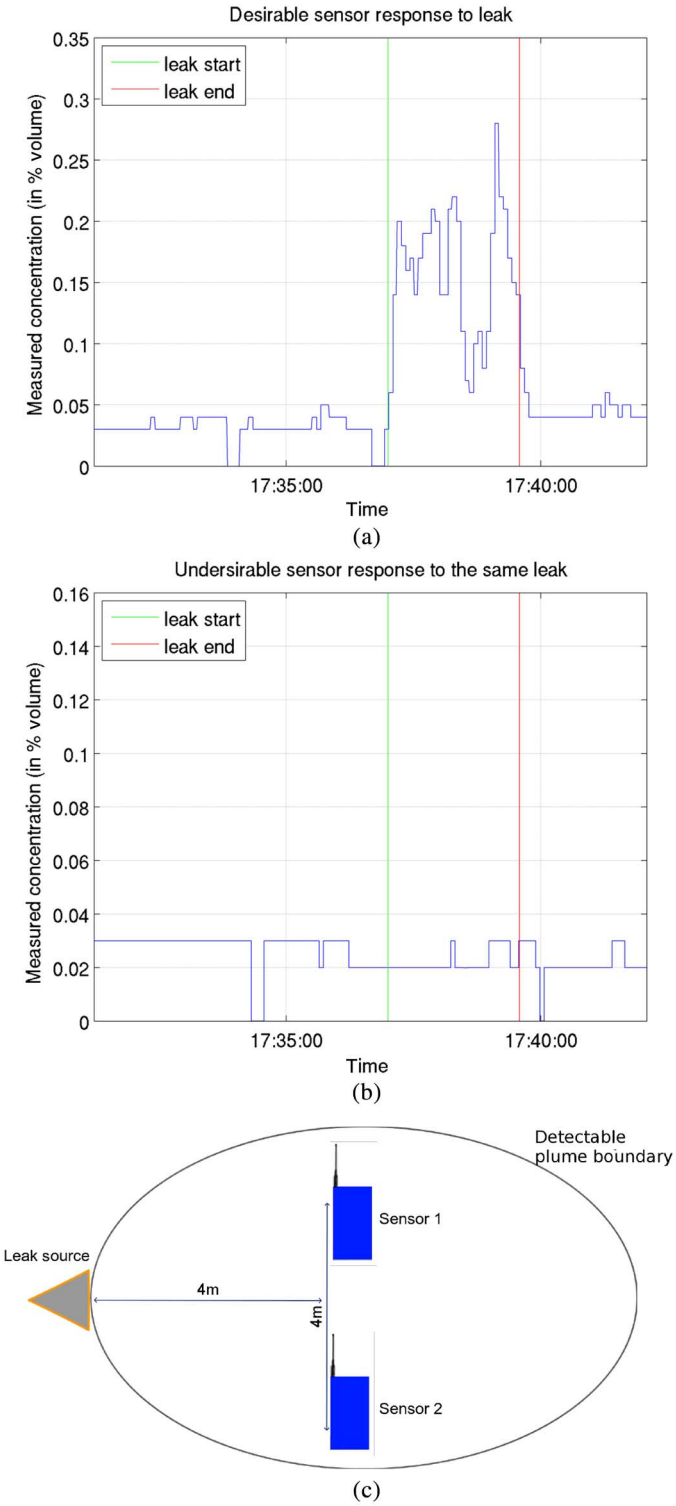


Fig. 2. Sensor SNR and response challenges: in this experiment, two sensors were positioned 4 m apart, and 4 m away from the source of the leak. These sensors were observed with an forward looking infrared (FLIR) camera and validated to be present in a detectable plume. (a) Sensor 1 response: even with a high noise floor, this sensor was responsive to the leak. (b) Sensor 2 response: elevated noise and no apparent response to the same leak. (c) Experimental setup diagram showing both sensors within the plume boundary during the leak.

based on the risk. To minimize the overall application energy consumption (for the entire system of sensors), neighboring devices might take turn in "guarding" a zone, then alerting

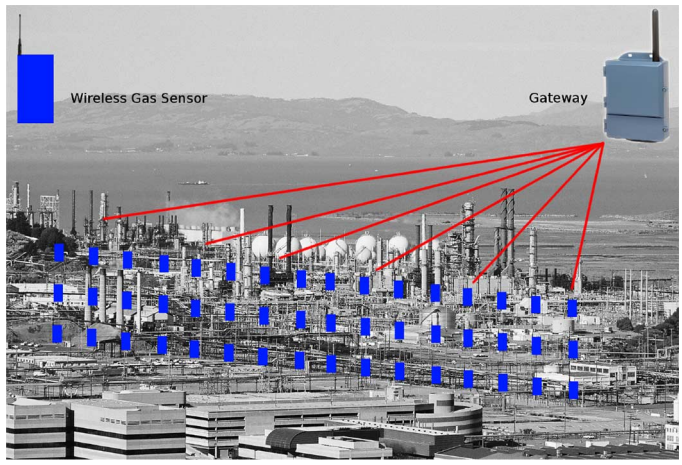


Fig. 3. Proposed system architecture: gas leak detection sensors are deployed extensively across a sensitive industrial area (a refinery in this case); data travel through the mesh network toward a single collection point (gateway) where the detection and localization algorithms are applied. The sensors can be duty-cycled spatially and temporally based on the measured concentrations.

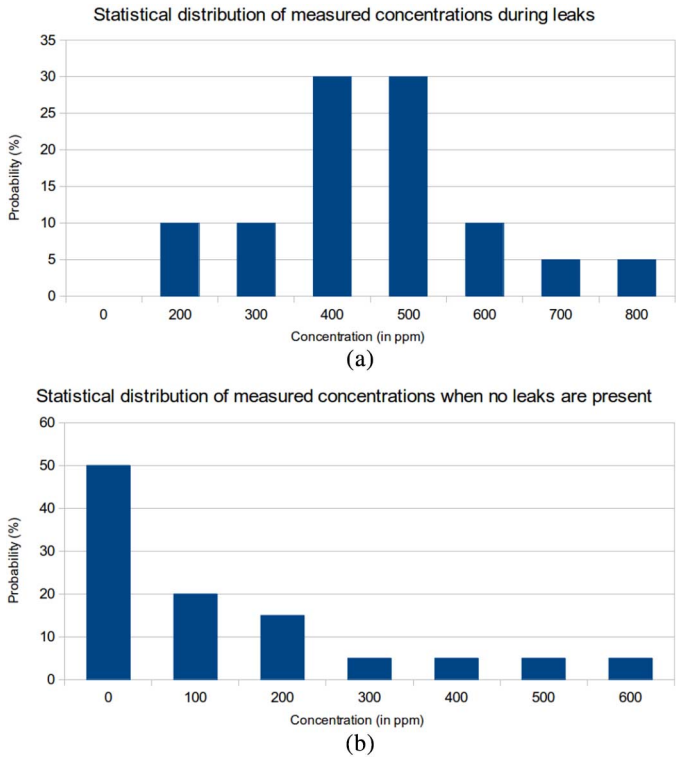


Fig. 4. Semiheuristic sensor model derived from experimental data. Noncomplementary probabilities accompany each state: ON (leak occurring) or OFF (no leak). This model was obtained by observing various sensor behaviors during leaks and in their absence (similar to the one shown in Fig. 2). The concentration counts were then performed and adjusted heuristically as shown in these histograms. As will be apparent, our detection method is based on the variations in probabilities in a particular period of time. (a) Sensor model for concentration measurements during a leak (ON Model). (b) Sensor model for concentration measurements during a leak (OFF Model).

the other devices in case of suspicious increase in measured concentrations.

Similar to having an adaptive spatial sampling of concentration, a temporal one would also be beneficial. This means that

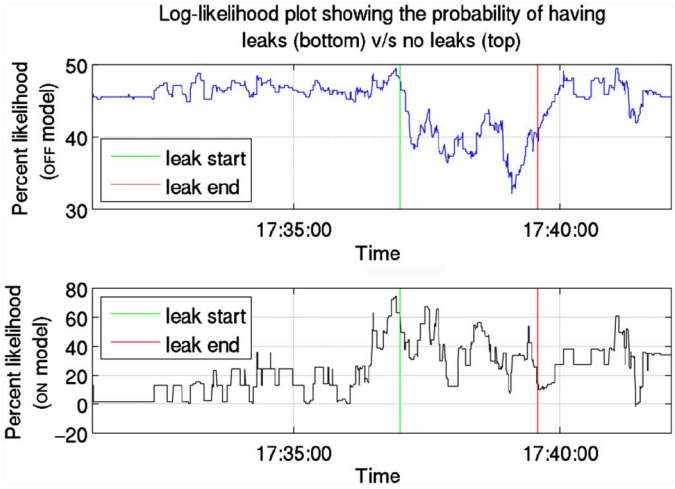


Fig. 5. Observation likelihood at each time step, for both states: as concentration measurements are received, the probability of having a leak versus no leak are computed. In the event of a gas release, one would expect to see the likelihood of having no leaks drop, while that of having leaks increase.

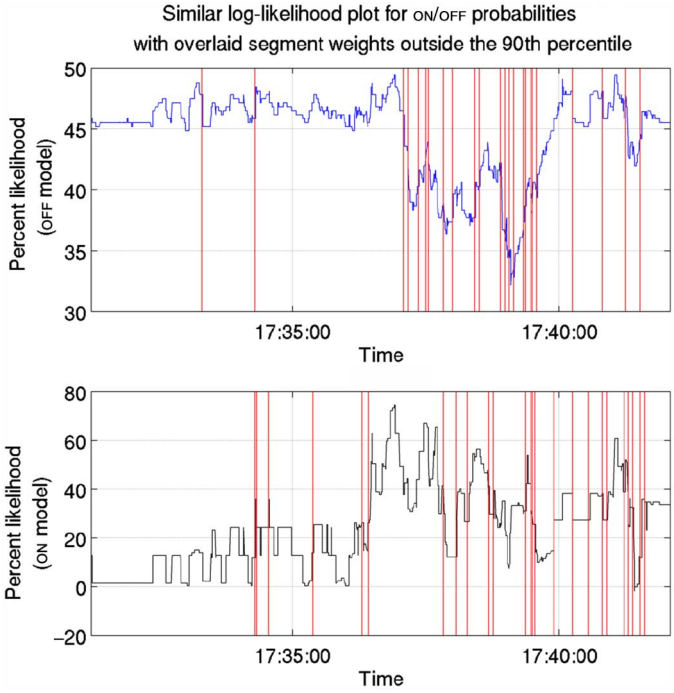


Fig. 6. Algorithm described here takes the likelihood time series as input and returns the instants in time where that plot went beyond the norm (by a certain percentile threshold).

the mote can decide to increase its sampling frequency when it detects a sudden surge in gas concentration. The reporting rate of data to the gateway, which is not very frequent regularly (on the order of one average reading every 10 min), can also be increased when the device records an unusual concentration of gas. Augmenting this method with a statistical routine can also get rid of many unnecessary alarms and minimize energy consumption. The experiments performed in this study were designed with oversampling. In long-term deployments, however, this large amount of data would not be necessary. Instead, sensor would transmit steady-state concentrations to the gateway in the form of averages and other statistical figures.

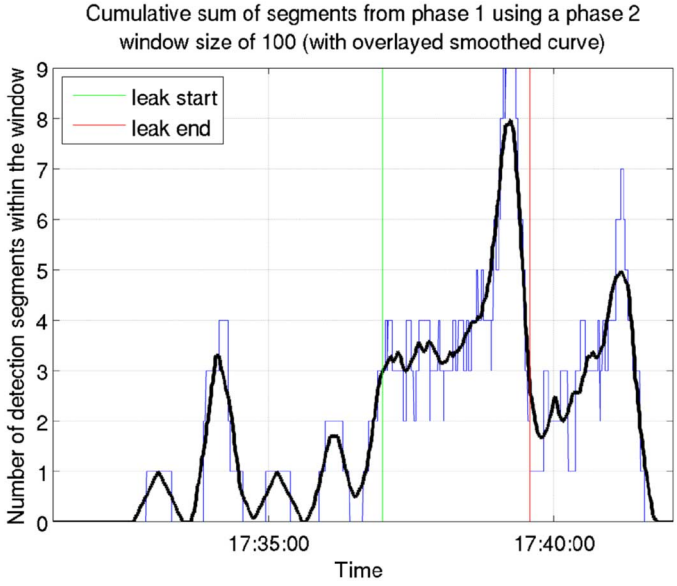


Fig. 7. Summing the detections in stage-2 allows for an easier identification of leaks. Depending on the window size, the amount of detections can cross a detection threshold for a considerable time. The summation plot, overlayed with a smoothed version for clarity is shown here.

As for the gateway, common practices involve powering it directly from the mains. However, it would be possible to utilize a solar scavenger with a rechargeable battery instead. Combined with a low-power Linux box, the WirelessHART gateway will consume on the order of 1.5 W on average.

### C. Detection Algorithm

Considering the system architecture above, where each sensor adaptively reports its gas concentration measurements to one location (through one or more gateways), we now look at a method for detecting the occurrences of leaks. Our framework is a probabilistic one, where each sensory observation $s(t)$ is represented probabilistically, then the total likelihood of a leak is computed at every time step. To get there, we model each sensor observation independently as $p(s_i(t)|\theta_t)$, where $i \in \{1, \ldots, M\}$, $M$ is the total number of sensors per area under consideration, and $\theta_t$ is an indicator variable, which represents the existence of a leak at time step $t$. We have derived semiheuristic models for our sensors both in the presence of a leak $(\text{ON}, \theta = 1)$ and when just measuring leak-free environments $(\text{OFF}, \theta = 0)$. The measurements and experiments leading to these models will be defined in Section IV. The histograms corresponding to the derived models are illustrated in Fig. 4.

Using these models, the likelihood at each time step is computed as follows:

$$L_t(\theta) = \prod_{i=1}^{N} p(s_i(t)|\theta). \tag{1}$$

When $\theta = 1$, we are essentially computing the likelihood of a leak being present (ON state). $L_t(\theta = 0)$ is the likelihood in the OFF state, or when no leaks are present. This is done at each time step, using all of the available sensory information $s_i(t)$ for $i \in \{1, \ldots, M\}$. Intuitively, one would expect

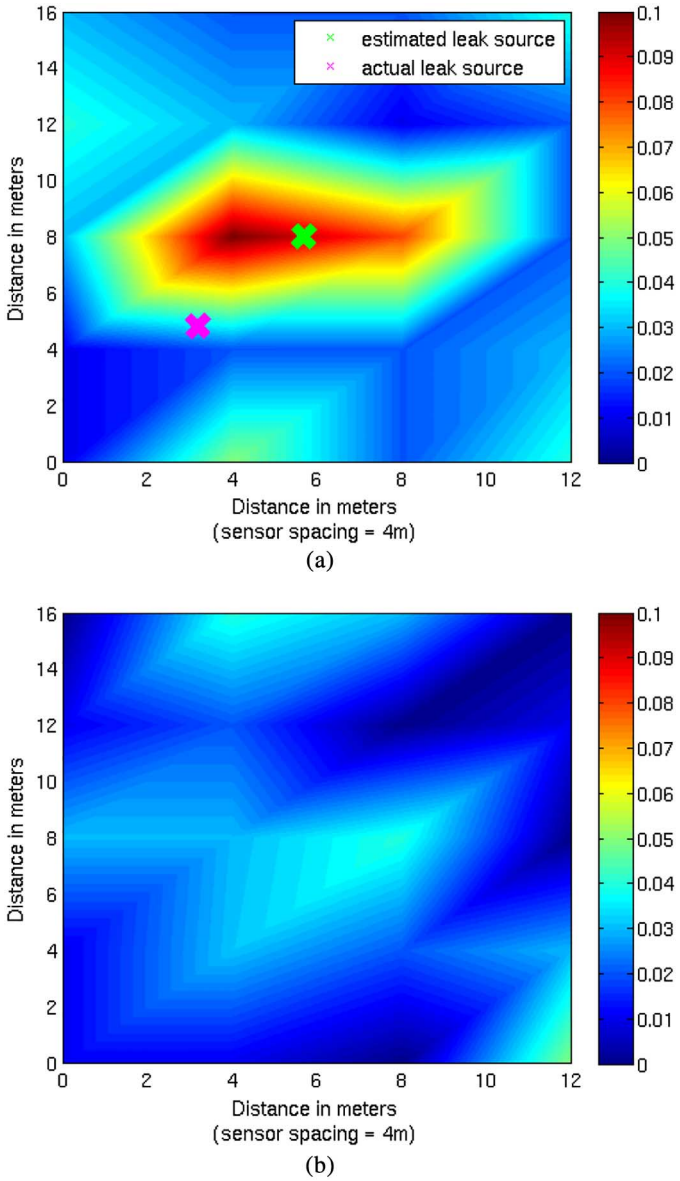


Fig. 8. Concentration heat maps of a 5 × 4 grid of sensors in two states: (a) during a leak; and (b) when no gas is present (the sidebar denotes concentrations in % volume).

$L_t(\theta = 1)$ to increase in the presence of a leak (i.e., ON state), while expecting $L_t(\theta = 0)$ to decrease during the same time. Such a behavior is observed in our experiments and Fig. 5 is one sample case.

In the quest for a completely automatic leak detection system, we would like to record these changes in the likelihood signal autonomously. We, therefore, treat the problem as a signal segmentation one [17]. In essence, we are interested in the segments of the likelihood time series, which differ from the normal. Such signal segmentation techniques have been successfully applied in electrocardiogram (ECG) and electroencephalogram (EEG) applications [18], [19]. We are using the algorithm presented in [18] to detect changes in our constructed likelihood signal $L_t(\theta)$, in both states. The method is detailed in Algorithm 1. The autocorrelation functions (ACFs) of segments of length $N$ are computed, as this windows progresses along the time series. Each ACF computation is called $A_i$, where $i \in \{1, \ldots, L/N\}$, and $L$ is the total length of the time series. The cosine of pair-wise ACF computations $(A_i, A_j | i \neq j)$ is performed, forming a similarity matrix of size $L/N \times L/N$. The weights of the similarity matrix are then calculated and indices outside of the $P$th percentile are labeled.

The main intuition behind this is the following: disturbance free segments of a signal should have *similar* ACFs. However, if there is a clear change in the signal, there should be a corresponding *dissimilarity* in the ACFs as well. Computing the pairwise cosine similarities between each ACF, one can visualize the similarity between the segments. By summing the columns of the resultant similarity matrix, the weights are computed. In our application, when there are no leaks, these weights are high. During a leak, however, we expect the weights to decrease, as they will be *dissimilar* to the regular 'no-leak' segments. The change in the segments is then detected simply by applying a threshold set at the $P$th percentile value.

The algorithm presented here then returns a number of time indices, which correspond to various regions of the likelihood series, which were unusual. We will name these time indices as stage-1 detections. Fig. 6 shows the same likelihood plots of Fig. 5, but with overlayed segments representing the stage-1 detections.

One of the important parameters of this algorithm is the percentile parameter. Depending on the percentile threshold, which is set, one can reduce the rate of false positives. These false positives arise from the fact that the sensor noise floors are elevated (as explained in part III-A), and therefore, reducing our signal-to-noise ratio (SNR). Increasing the percentile threshold in our algorithm reduces the false alarm rate, but this, however, comes at the price of a reduction in true positives. This parameter should be, therefore, set in such a way that *alarm fatigue* and a "tolerable" leak miss rate are balanced.

**Algorithm 1.** Phase-1 change detection algorithm

1: **Input**: likelihood timeseries, window size $N$, percentile value $P$
2: **Output**: indices of the segments corresponding to the irregularities
3: Segment the signal into epochs of length $N$
4: Compute the Auto-Correlation Functions (ACFs) of each segment, $A_i$
5: Compute the cosine similarity between each pair of ACFs

$$\cos \sigma_{ij} = \frac{A_i^T A_j}{\|A_i\| \, \|A_j\|} \tag{2}$$

and form the similarity matrix
6: Compute the weights by summing the columns of the similarity matrix
7: Calculate the $P$-th percentile of the weights
8: Label the segments with weights outside the $P$-th percentile

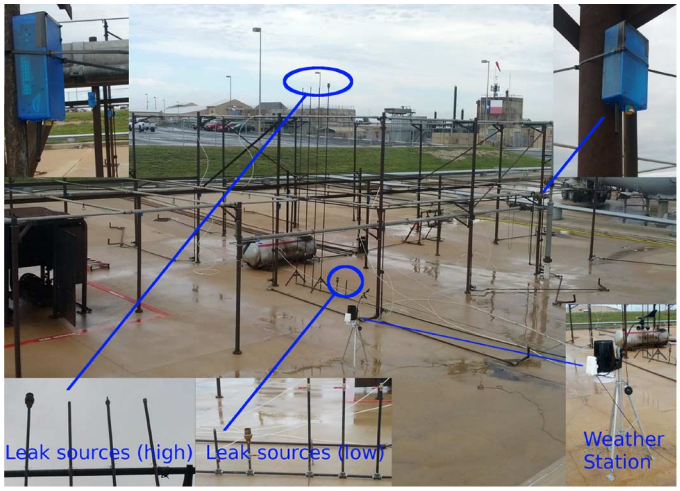


Fig. 9. Site of the experiment in College Station, TX. This figure shows the two release points and the placement of the 20 sensor grid ($5 \times 4$) at an elevation of about 2.25m.

Another effect of the sensor noise is the fact that some of the stage-1 detections actually correspond to fluctuations of concentration measurements triggered by temperature variations around the sensing element. This explanation was obtained from the sensor manufacturer. This effect means that we are not able to immediately consider the output of the first stage and have to perform additional steps before making a decision. To reduce *false positives*, we look at the total number of stage-1 detections in a sliding window. A sample output of stage-2 is shown in Fig. 7, where a window size of 100 was utilized. If this cumulative count of detections exceeds some predetermined threshold level for a preset period of time, we then output a detection, which we name as stage-2 detection. The length of the sliding window, the threshold level, and the duration of crossing can all be used to control the false positive and true positive rates, similarly to stage-1. The overall performance of stage-2 detections (and therefore, that of the entire algorithm) is analyzed with respect to user-set parameters (percentile threshold, stage-1 window size, and stage-2 window size). The results are presented in Section IV.

### D. Localization Algorithm

Following a successful detection of a leak by both stages of the algorithm, a localization routine is called. We utilized a simple center of mass approach. Upon finding a detection, we calculate the two-dimensional mean of the concentration measurements in the $X-Y$ plane

$$\hat{x} = \frac{\sum_{i=1}^{N} s_i(t) x_i}{\sum_{i=1}^{N} s_i(t)} \tag{3}$$

$$\hat{y} = \frac{\sum_{i=1}^{N} s_i(t) y_i}{\sum_{i=1}^{N} s_i(t)}. \tag{4}$$

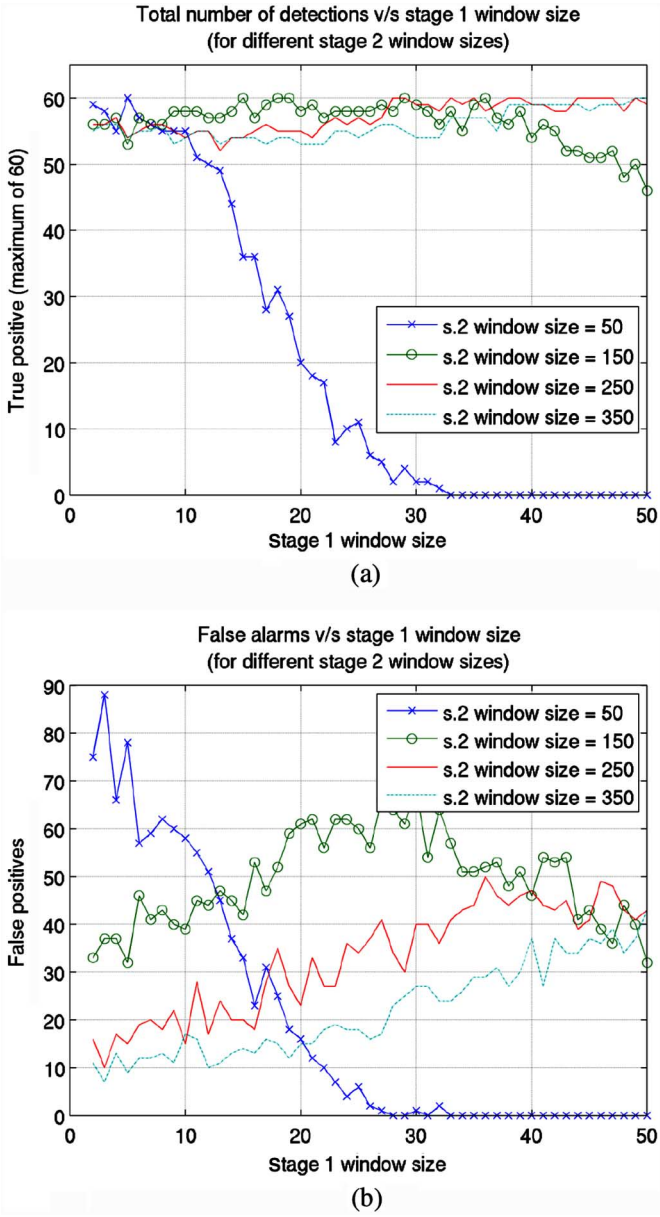


Fig. 10. Impact of varying the stage-1 window size on the number of detections and false alarms. (a) An increase in the window size generally leads to a decrease in the number of detections. (b) False alarms also increase with the window size.

In the above equations, $x_i$ and $y_i$ represent the coordinates of each sensor, whereas $s_i(t)$ is the sensor concentration reading. The resulting point $(\hat{x}, \hat{y})$ is defined as the estimate of the leak source detection. This would correspond to find the point of maximum concentration on a heat map. Fig. 8 depicts the localization result on a particular heat map.

### E. Possible Improvements to Our Method

In our analysis, we assumed that the sensory readings are conditioned only on the state of the leak (i.e., ON vs. OFF). Now, as the deployment grows in size, a far-away sensor from the leak source will probably not be able to detect any change. Still, considering a reduced spatial sampling, the response of the sensor to the plume of gas will depend on its location with respect to

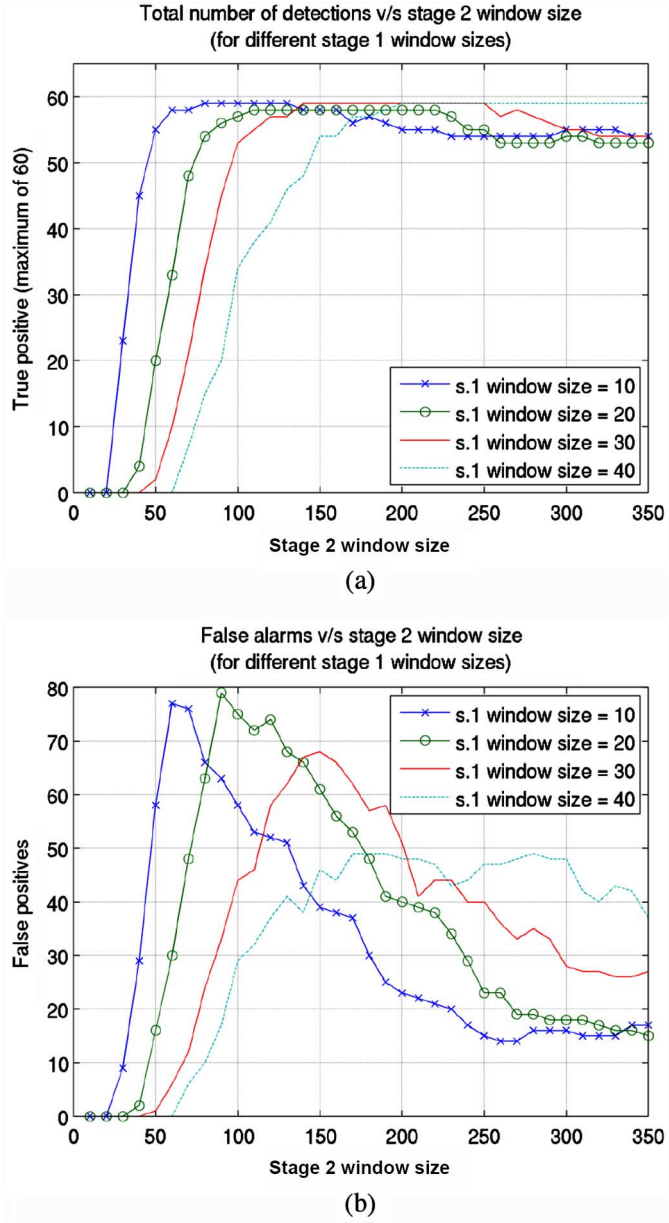


Fig. 11. At the second stage, a larger window size tends to have a better performance overall. (a) Increase in window size beyond a certain point reduces the number of detections by a small number. (b) False alarms are reduced when the stage-2 window size is larger.

this plume. To take this into account, the sensor models would be augmented in the following form:

$$p(s_i(t)|\theta, \text{location}). \tag{5}$$

However, developing sensor models based on plumes is well beyond the scope of this work, and it would somehow complicate the study. Nevertheless, it is worth mentioning that a location-dependent model can be worked out similarly to the previous section. The likelihood methods will then be directly applied, with some tuning.

Other important improvement that can be introduced is time dependence. With our current approach, we do not exploit the fact that if a leak exists at time $t$, it is then likely for this leak to remain at time $t+1$. Considering this feature means that we could use a general state space model to describe the leak phenomenon. Our objective would then be to perform state estimation, for which one may resort to Kalman filtering, unscented Kalman filtering, or particle filtering.

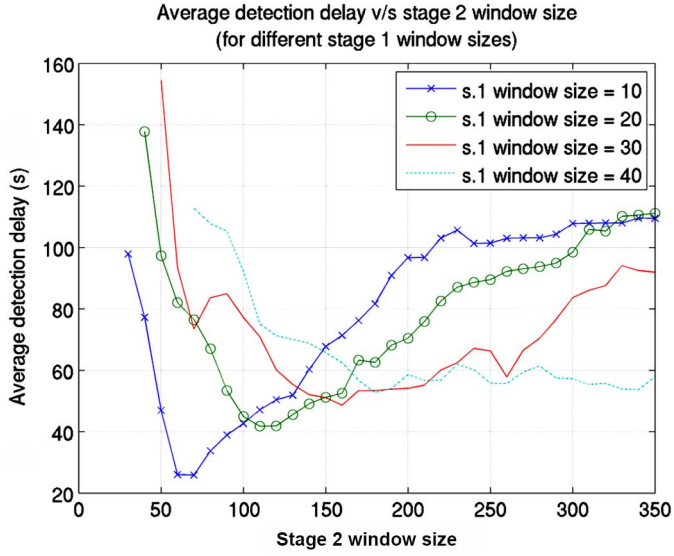


Fig. 12. Stage-2 window size increase leads to a decrease in false alarms, but that comes at the expense of an increase in detection delay.

## IV. Experimental Validation

To validate our architecture, hardware, and algorithms, we took part in an experiment at the Texas A&M Engineering Extension Service facility, College Station, TX, USA. Over the period of 3 days, more than 60 propane leaks of 2 min each were released. These leaks were monitored using the detection system presented here, and controlled by a team of engineers and a team of firefighters. The site of the releases is shown in Fig. 9. Twenty wireless propane sensors were used to monitor an area of about 200 $\text{m}^2$ surrounding the two release points (at 0.5 and 5.5 m). The sensors were placed in a $4 \times 5$ grid configuration, with a separation of about 4 m. All of them were mounted on an elevation of about 2.25 m. These devices measured propane concentrations at a rate of one measurement every 5 s. The measurements were collected in a data packet and transmitted to a nearby gateway. We now present the results of our algorithm applied to 60 releases of different source heights, source nozzle sizes (2, 6.35, 19, and 63.5 mm), and flow rates (ranging between 1.35 and 1020 lb/h).

### A. Detection Results

The algorithms described in Section III were applied to the collected concentration measurements, with different parameters modified for every pass. First, we look at the number of correct detections and false alarms as the stage-1 window size is varied. The results are shown in Fig. 10. The general trend observed shows that increasing the window size of the first stage does not affect the number of detections greatly, except when it grows to a point where the actual variations

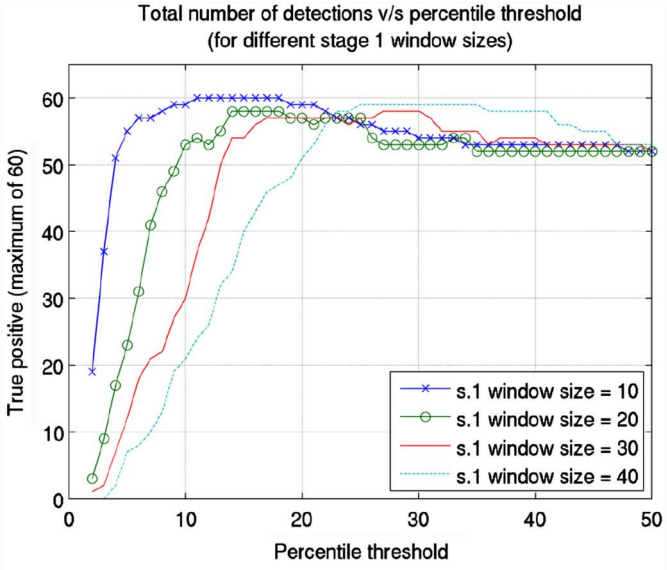


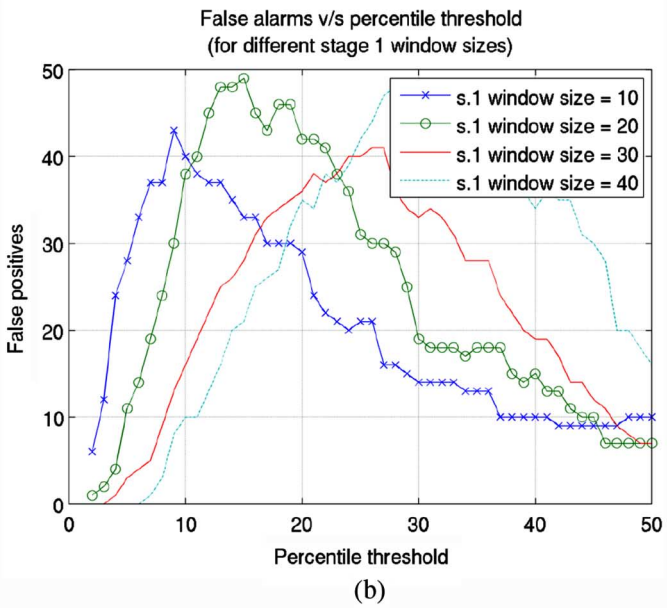


Fig. 13. Percentile threshold parameter is very important in determining the performance of these routines. (a) Percentile threshold in the 10%–20% seems to lead to a higher number of detections. (b) Number of false alarms rises quickly with the percentile, before it rolls off at a slower rate.

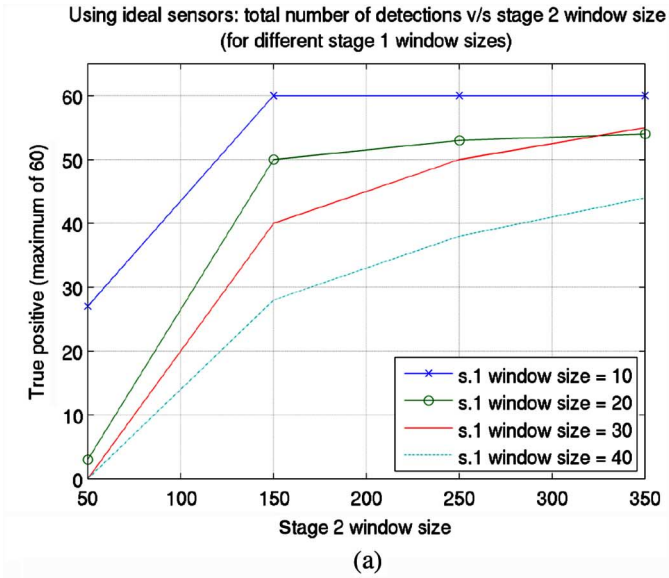


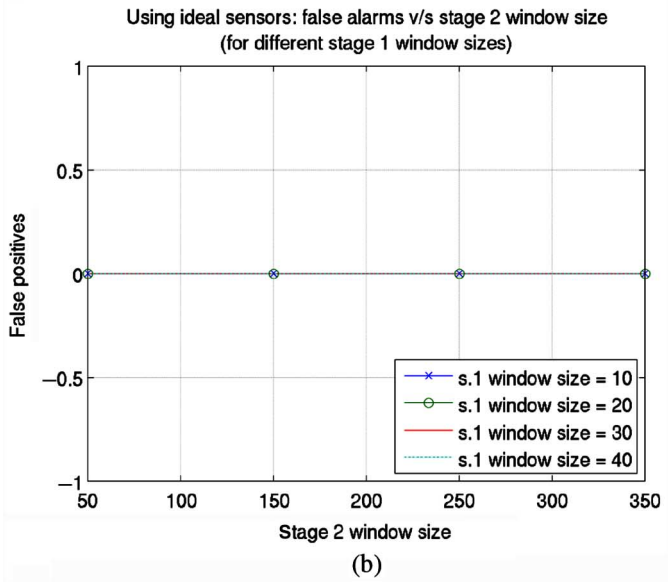


Fig. 14. Given ideal sensors (with enhanced SNR), the detection problem would become much easier. This plot shows the result of the two-stage detection algorithm presented here applied to 'ideal' data generated from the experimental one. (a) In some configurations, detecting all of the releases becomes possible. (b) Rate of false alarms is zero across most configurations.

associated with the leaks are no longer beyond the selected percentile threshold. This effect is accelerated when the window size of stage-2 is reduced. The effect in question is readily visible in Fig. 10(a) for the stage-2 window size of 50. Looking at false positives, we notice that the trend peaks at a particular stage-1 window size before starting to roll off. However, it is to note that this roll-off is sometimes associated with a reduction in detections as well.

The impact of changing the stage-2 window size on the number of true and false positives is shown in Fig. 11. Concerning the number of detections, increasing the size of the stage-2 window shows an increase in these detections, which tends to settle (with a slight dip) beyond a particular point (around 125 samples). At the same time, the number of false alarms increases sharply before it peaks and decreases with an increasing window. This validates the conjecture made before: increasing the stage-2 window size allows us to have a better detection methodology, as it decreases the number of false alarms, while not diminishing the true positives much.

However, and as expected, increasing the stage-2 window size has a direct effect on delays. This is readily observed in Fig. 12. Though the delay starts by being elevated with short window sizes, this can be explained by the fact that the number of leaks detected with that configuration is very low, and the data are, therefore, not representative. However, once the delay reaches a minimum value, it starts to climb back up with increased stage-2 window size. Indeed, the confidence in the

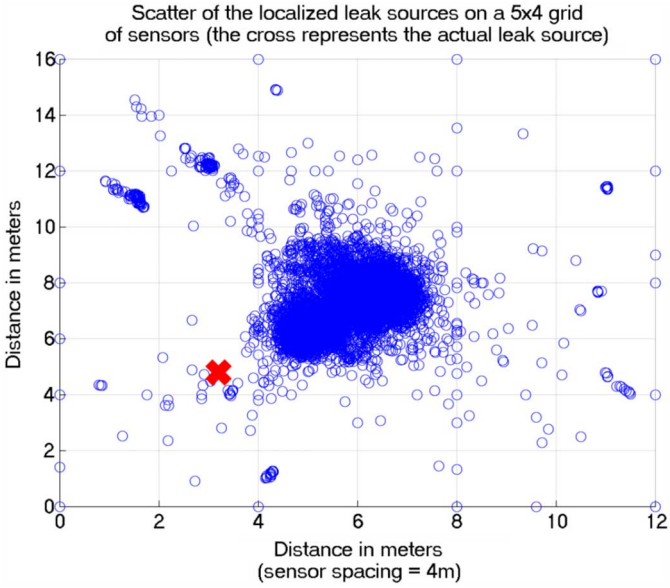


Fig. 15. Scatter plot of all of the detections (during many different configurations). The offset seen between the real source of the leak and the conglomeration of detections could be explained by the fact that no sensors were present directly above the source.

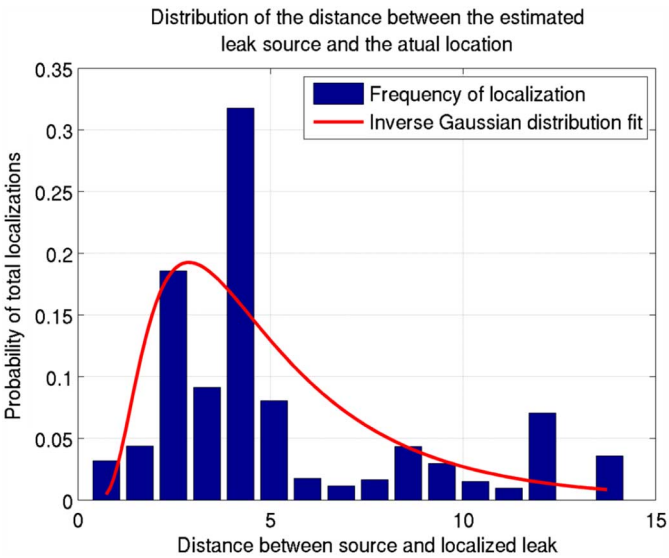


Fig. 16. Histogram of the distances between the detections and the real source of the leak is shown. More than 50% of all detections are within 3 m of the source.

detection increases, but the consequence is that the algorithm has to wait for more and more samples before making the decision.

As explained before, the percentile parameter is an important one that determines the performance of our detection method. Looking at Fig. 13, we notice that increasing this parameter has a similar effect in increasing the stage-2 window size: the number of detections rises quickly before starting to dip slightly with increase in percentile threshold, while the number of false alarms rises quickly in the beginning, before dropping, as the percentile is increased.

At this point, it is worth noting that the most balanced configuration of this algorithm returned a detection rate of

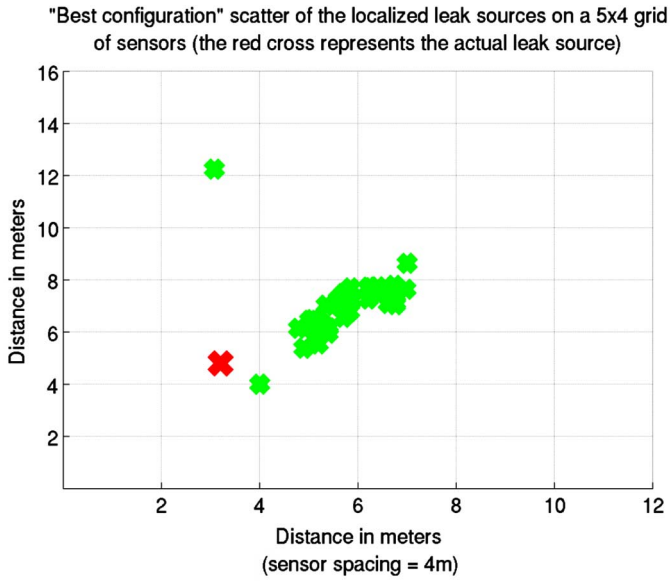


Fig. 17. In the preferred configuration (resulting in 55 detections out of 60, with seven false alarms), the localization results appear even closer to the actual source of the leaks.

55/60, with seven false alarms, and an average delay of 108 s. Though these results seem promising, they leave a lot of room for improvement. The detection rate is satisfactory, especially when compared to the absence of widespread reliable detection methods on the market today, but a 100% rate would be desirable of course. A delay of more than 100 s could represent some challenges for a refinery workers in responding to an alarm, so reducing it to below 1 min is also desired. Finally, a false alarm rate of 7 over a period of 3 days seems excessive, even if these alarms were short-lived. Still, a false-positive rate of 1 per plant per month (or per year) would be highly desirable, especially with an elevated detection rate to accompany it. To reach these desirable results, we would require an improvement in sensor technology of at least one order of magnitude in SNR. Concerning the lifetime of the sensors, and to enable a 10-year deployment without the need to change batteries, a reduction in power consumption of two orders of magnitude is required for reliable detection.

With this in mind, we "massage" our experimental data to reduce its noise as proposed and run the algorithm again. The results are shown in Fig. 14. It is clear that certain configurations of our detection methodology would give us a 100% detection rate (while others give a slightly reduced rate). Most important, however, is the false alarm rate, which stays at zero across all configurations considered here.

## B. Localization Results

We now look at the localization results, given our noisy sensors covering the test site. Upon finding a detection, the center of mass routine is called upon the concentration data, and the point of highest mean in both the $X$ and $Y$ directions is identified as the leak source estimate. Fig. 15 shows a scatter of these detection estimates (for different parameters described above)

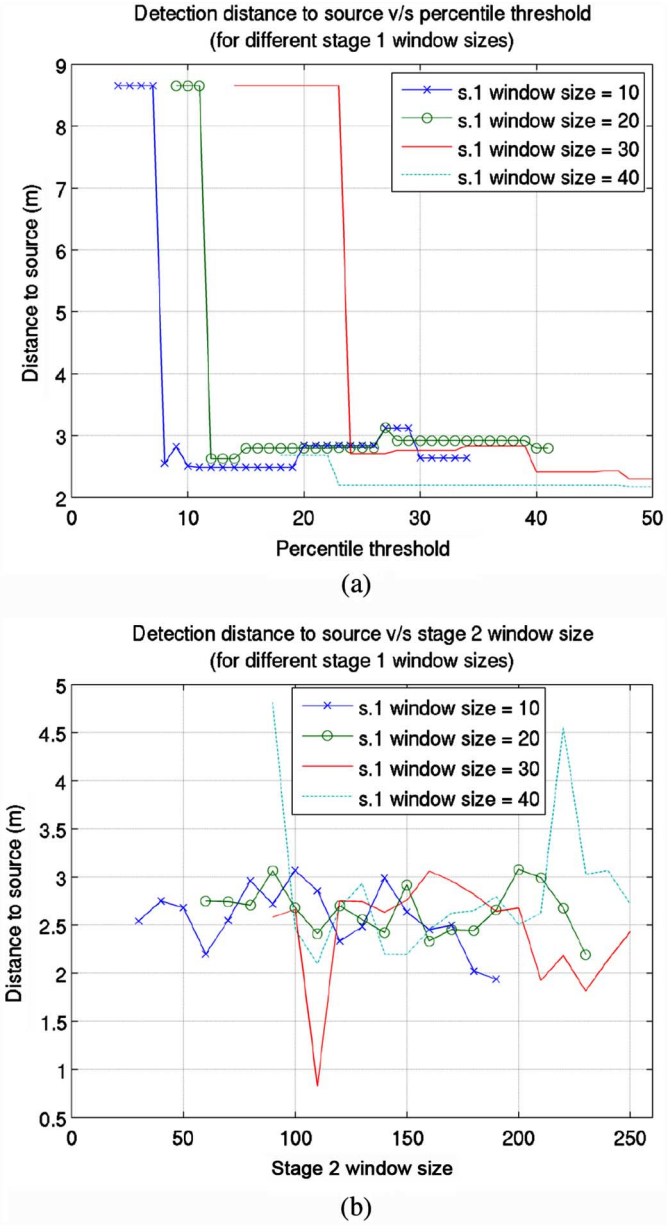


Fig. 18. Distance between the detected leak and the real source, for one particular release under various algorithm configurations. (a) Larger percentile thresholds tend to yield better localization results since the response of more sensors is taken into account. (b) Stage-1 and stage-2 window sizes largely do not affect the localization.

along with the true source of the leaks. Most of the detections seem clustered in the middle of the sensor grid, but with a slight skew toward the actual source. One potential explanation to this phenomenon is the absence of sensors directly above the leak release point. This means that the algorithm is converging toward the closest sensor(s) in the vicinity of this source.

Looking at the distribution of distance between the estimated leak source and the actual one in Fig. 16, we can see that it follows an inverse Gaussian trend. Most detections actually occurred less than 3 m away from the leak source, and a striking majority were localized less than 5 m away. The localizations of the 55 "best" detections, which were obtained as described above (with the seven false alarms and the delay of 108 s), are shown in Fig. 17. Finally, Fig. 18 shows the distance between the detected leak and the actual source, for one particular leak and across different configurations. Larger percentile thresholds lead to better detections since the concentration measurements of more sensors are taken into account. In general, varying the stage-1 and stage-2 window sizes does not affect the localization results greatly. The main reason is that the localization routine is purely a center of mass approach, and should not be affected by the parameters. Hence, unless the detection is distant, localization results will be more or less independent of configuration parameters. However, by looking at particular leaks, some configurations were identified as problematic across various gas releases. The results shown confirm the reliability of the localization method, with no estimates found in unusual locations (near the edge of the network). In a realistic deployment, the localization figures presented here would be very helpful for workers who are familiar with the equipment present in the vicinity of the sensors, and who should quickly be able to identify the source of the leak.

## V. Conclusion

In this study, we proposed, implemented, and validated a wireless distributed gas leak solution for industrial places. In our system architecture, many gas sensors are placed around a region of interest in a plant, and they all report to a single location. These sensors are duty-cycled in time and space to conserve energy (as they are battery powered). At the gateway, an algorithm is run on the measured concentration data, which allows the detection and localization of the leaks. In our experiment (with 20 sensors and a monitoring area of 200 $\mathrm{m}^2$), we were able to detect 55 out of the 60 releases, with an average delay of 108 s, and a localization accuracy under 5 m. Over the period of 3 days, we saw seven false alarms. Though we can achieve these results nowadays, there is still some work to be done to get this idea into productization. In this study, we made an attempt at being as agnostic to the leak source as possible. Studying the relationship between flow rates and nozzle sizes would be beneficial and is left for future research. As the wireless communication reaches new boundaries in reliability, and as efficient microcontrollers become cheaper and less power hungry, the only component left to be improved is the sensor. Certainly, improvements on the detection algorithm could help reduce the false alarm rate and increase the detection rate, but the sensing hardware would be a better place to start. An order of magnitude improvement in signal to noise needs to be accomplished in explosive gas sensors (to reduce false alarms). A faster wake-up and quicker response time is required for faster detections. Finally, two orders of magnitude of improvement in energy consumption is needed to extend the lifetime of the device to 5 years. As a concluding note, and though this study was done with industrial plants in mind, we feel that similar approaches can be accomplished in cities of the future, where a gas detection and localization system can help address the problems of leaks in urban gas pipelines.

## ACKNOWLEDGMENT

The authors would like to the Texas A&M Engineering Extension Facility and their helpful staff, and the Texas A&M team led by Dr. Y. Liu. Finally, they would like to acknowledge B. Coleman and J. Cedeno for driving crucial change in today's corporate world.

## REFERENCES

[1] Directed Inspection and Maintenance at Gas Processing Plants and Booster Stations, United States Environmental Protection Agency, BiblioGov 2013, ISBN 978-1288576357.

[2] United States Environmental Protection Agency. "Industry sector emissions," United States Environmental Protection Agency, retrieved on Aug. 2014[Online]. Available: http://epa.gov/climatechange/ghgemissions/sources/industry.html

[3] D. Gurney, D. Alleman, and T. Kulp, "Development of hydrocarbon vapor imaging system for petroleum and natural gas fugitive emission sensing," National Energy Technology Laboratory (NETL), Office of Fossil Energy, United States Department of Energy, Feb. 2004.

[4] G. Laframboise and B. Karschnia, "Improve exploration, production and refining with 'add-at-will' wireless automation," *Hydrocarbon Process.*, vol. 14, no. 10, pp. 35–38, 2010.

[5] U.K. Health, and Safety Executive, *The Selection and Use of Flammable Gas Detectors*. U.K.: U.K. Health and Safety Executive, 2004 [Online]. Available: http://www.hse.gov.uk/pubns/gasdetector.pdf, accessed on Jan. 2015.

[6] P. Murvay and I. Silea, "A survey on gas leak detection and localization techniques," *J. Loss Prev. Process Ind.*, vol. 25, pp. 966–973, 2012.

[7] X. Liu *et al.*, "A survey on gas sensing technology," *Sensors*, vol. 12, pp. 9635–9665, 2012.

[8] E. Sizeland, "Ultrasonic devices improve gas leak detection in challenging environments," *World Oil*, vol. 20, pp. 133–135, Oct. 2014.

[9] R. T. Kester, "A real-time gas cloud imaging camera for fugitive emission detection and monitoring," *Imag. Appl. Opt. Tech. Pap.*, 2012, doi: 10.1364/AIO.2012.AW1B.1, 2012.

[10] S. So, F. Koushanfar, A. Kosterev, and F. Tittel, "LaserSPECks: Laser SPECtroscopic trace-gas sensor networks—Sensor integration and applications," in *Proc. 6th Int. Symp. Inf. Process. Sens. Netw. (IPSN'07)*, Apr. 2007, pp. 226–235, ISBN 978-1-59593-638-7.

[11] A. Somov *et al.*, "Energy-aware gas sensing using wireless sensor networks," in *Wireless Sensor Netw.*, vol. 7158. 2012, pp. 245–260.

[12] G. T. Nofsinger and K. W. Smith, "Plume source detection using a process query system," in *Proc. Defense Secur. Symp. Conf.*, Bellingham, WA, USA, 2004.

[13] J. Huseynov, S. Baliga, N. Bagherzadeh, L. Bic, and M. Dillencourt, "Gas-leak localization using distributed ultrasonic sensors," in *Proc. 16th SPIE Conf. Smart Sens. Phenom. Technol. Netw. Syst. II*, San Diego, CA, USA, 2009.

[14] J. Weimer, B. Sinopoli, and B. H. Krogh, "Multiple source detection and localization in advection-diffusion processes using wireless sensor networks," in *Proc. 30th IEEE Real-Time Syst. Symp. (RTSS)*, 2009, pp. 333–342.

[15] F. Chraim and K. Pister, "Wireless valve position monitoring: A MEMS approach," in *Proc. 39th Annu. Conf. IEEE Ind. Electron. Soc.*, 2013, pp. 4016–4021.

[16] F. Chraim and K. S. J. Pister, "Smart fence: Decentralized sequential hypothesis testing for perimeter security," in *Sensor Syst. Softw.*, vol. 122. 2013, pp. 65–78, 978-3-319-04165-0.

[17] M. Lavielle, "Optimal segmentation of random processes," *IEEE Trans. Signal Process.*, vol. 46, no. 5, pp. 1365–1373, May 1998.

[18] C. Varon, D. Testelmans, B. Buyse, J. Suykens, and S. Van Huffel, "Robust artefact detection in long-term ECG recordings based on autocorrelation function similarity and percentile analysis," in *Proc. Annu. Int. Conf. IEEE Eng. Med. Biol. Soc. (EMBC)*, 2012, pp. 3151–3154.

[19] P. Micó, M. Mora, D. Cuesta-Frau, and M. Aboy, "Automatic segmentation of long-term ECG signals corrupted with broadband noise based on sample entropy," *Comput. Methods Prog. Biomed.*, vol. 98, no. 2, pp. 118–129, 2010.

**Fabien Chraim** received the Bachelor's degree (hons.) in electrical and computer engineering from the American University of Beirut, Beirut, Lebanon, in 2009, and the M.S. and Ph.D. degrees in civil systems engineering and electrical engineering and computer sciences, respectively, in 2010 and 2014, from the University of California, Berkeley, CA, USA.

He was a Student Researcher with the Berkeley Sensor and Actuator Center, working with Prof. Kristofer S.J. Pister. He is the Chief Technology Officer and Co-Founder of Solfice Research, Inc., Berkeley, CA, USA.

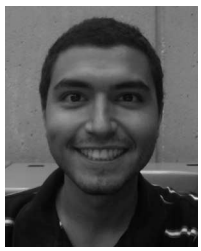

**Yusuf Bugra Erol** received the B.S. degree (rank 1) in electrical engineering from the Middle East Technical University (METU), Ankara, Turkey, in 2011. He is currently pursuing the Ph.D. degree at the University of California, Berkeley, CA, USA, working with Prof. Stuart Russell.

His research interests include combined state and parameter estimation for nonlinear and non-Gaussian dynamic models using sequential Monte-Carlo methods and their application to medical monitoring.

**Kristofer S. J. Pister** received the B.A. degree in applied physics from the University of California, San Diego (UCSD), La Jolla, CA, USA, in 1986, and the M.S. and Ph.D. degrees in electrical engineering from the University of California–Berkley (UCB), Berkeley, CA, USA, in 1989 and 1992, respectively.

He was an Assistant Professor with the Department of Electrical Engineering, University of California–Los Angeles (UCLA), Los Angeles, CA, USA, from 1992 to 1997, where he coined the phrase Smart Dust. Since 1996, he has been a Professor of Electrical Engineering and Computer Sciences at UCB. From 2003 to 2004, he was on leave from UCB as Chief Executive Officer and then Chief Technology Officer of Dust Networks, a company he founded to commercialize wireless sensor networks. He participated in the creation of several wireless sensor networking standards, including Wireless HART (IEC62591), IEEE 802.15.4e, ISA100.11A, and Internet Engineering Task Force IPv6 Routing Protocol for Low-Power and Lossy Networks (IETF RPL). He has participated in many government science and technology programs, including Defense Advanced Research Projects Agency Information Science and Technology (DARPA ISAT) and the Defense Science Study Group, and he is currently a Member of JASON. His research interests include microelectromechanical systems, microrobotics, and low power circuit